

Photoprotons Produced by 245 ± 15 -Mev Gamma Rays on Carbon*

ROBERT J. CENCE AND BURTON J. MOYER

Lawrence Radiation Laboratory, University of California, Berkeley, California

(Received January 23, 1961)

A carbon target was bombarded by 342-Mev bremsstrahlung from the Berkeley synchrotron. The energy spectrum of protons produced at 60 deg was measured from 90–250 Mev. Interactions due to 245 ± 15 Mev gamma rays were selected out by requiring a coincidence between the protons from the target and the electrons associated with these gamma rays. Analysis was made using the quasi-deuteron model of Levinger. In contrast with previous analyses of this kind, conservation of both momentum and energy were taken into account in a fairly accurate way. Results of this analysis determine the momentum distribution of the centers of mass of the quasi-deuterons. The momentum distribution that results in the observed proton spectrum, normalized to one quasi-deuteron, is given by

$$\frac{d^2N}{dP_D^3} = \frac{0.2}{(4\pi ME_1)^{1/2}} \exp\left(-\frac{P_D^2}{4ME_1}\right) + \frac{0.8}{(4\pi ME_2)^{1/2}} \exp\left(-\frac{P_D^2}{4ME_2}\right),$$

where $E_1 = 1.6$ Mev, $E_2 = 20$ Mev.

I. INTRODUCTION

MANY experimenters have measured the energy distribution of photoprotons produced by high-energy gamma rays on light nuclei.^{1,2} The most dominant feature of this distribution is the large number of high-energy protons produced at small angles. This was interpreted by Levinger to mean that the incoming photons interact with a small subunit in the nucleus—in particular, a neutron-proton pair which he called a quasi-deuteron.³ In this model, a neutron and a proton are simultaneously ejected from the nucleus. The mechanism of this interaction, although similar to that of photodisintegration of the deuteron, is modified by the momentum distribution of the quasi-deuterons in the nucleus. Levinger showed that in this process the neutron and proton pair must be in close proximity. Under this condition, the wave function of the quasi-deuteron is just a multiple of that of the free deuteron. This interaction is therefore approximately proportional to the photodisintegration cross section of the free deuteron, suitably averaged over the momentum distribution of the quasi-deuterons.

The basic validity of this model has been verified by observing conjugate neutrons and protons in coincidence.⁴ It is thus possible to use this model to calculate the momentum spectrum of neutron-proton

pairs in the nucleus from the measured energy spectrum of ejected photoprotons.

It must be pointed out that detailed experimental comparison with the theory is not easily obtained. This is because high-energy photon beams are produced by bremsstrahlung of electrons, so that the gamma rays have a continuous spectrum of energies with approximately a $1/E$ dependence. This has the effect of smoothing out the proton spectrum and masking the details of the interaction.

In order to gain more detailed information, Weil and McDaniel in 1953 attempted to select out gamma rays in a small energy interval.² They developed a technique to observe the spectrum of protons from carbon due to 190-Mev gamma rays. However, the energy resolution obtained was rather broad (± 30 Mev), and furthermore, the electronic apparatus was very complicated because they were trying to attain time resolutions not then easily obtainable. They concluded it would probably have been as well to perform the experiment by successively reducing the energy of the accelerator and using the subtraction technique.

Since the experiment of Weil and McDaniel, counting techniques have developed to such an extent that coincidence-resolving times of a few millimicroseconds

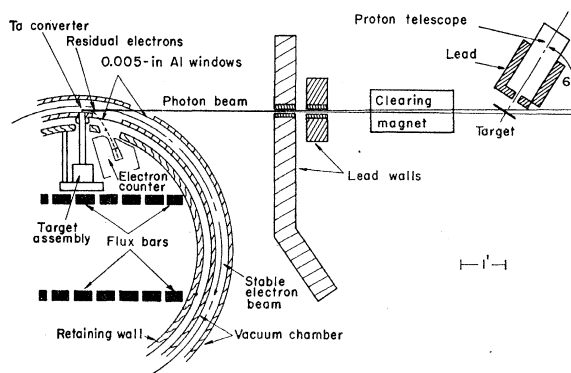


FIG. 1. Plan view of the experimental setup.

* This work was done under the auspices of the U. S. Atomic Energy Commission.

¹ D. Walker, Phys. Rev. **81**, 634 (1951); C. Levinthal and A. Silverman, *ibid.* **82**, 822 (1951); J. C. Keck, *ibid.* **85**, 410 (1952); J. W. Rosengren and J. M. Dudley, *ibid.* **89**, 603 (1953); B. T. Feld, R. D. Godbole, A. Odian, F. Scherb, P. C. Stein, and A. Wattenberg, *ibid.* **94**, 1000 (1954).

² J. W. Weil and B. D. McDaniel, Phys. Rev. **92**, 391 (1953).

³ J. S. Levinger, Phys. Rev. **84**, 43 (1951).

⁴ M. Q. Barton and J. H. Smith, Phys. Rev. **95**, 573 (1954); H. Myers, A. C. Odian, P. C. Stein, and A. Wattenberg, *ibid.* **95**, 576 (1954); R. Weinstein, A. C. Odian, P. C. Stein, and A. Wattenberg, *ibid.* **99**, 1621 (1955); A. C. Odian, P. C. Stein, A. Wattenberg, B. T. Feld, and R. Weinstein, *ibid.* **102**, 837 (1956); A. Wattenberg, A. C. Odian, P. C. Stein, H. Wilson, and R. Weinstein, *ibid.* **104**, 1710 (1956); M. Q. Barton and J. H. Smith, *ibid.* **110**, 1143 (1958).

with high efficiency and electronic stability are readily available. For this reason, we thought it was worth while to attempt another experiment with selected gamma rays.

II. EXPERIMENTAL METHOD

This experiment was performed at the Berkeley synchrotron. The experimental arrangement is shown in Fig. 1. The photon beam was produced by the 342-Mev electron beam striking a 0.0013-in. tantalum target. Photon selection was made by an electron

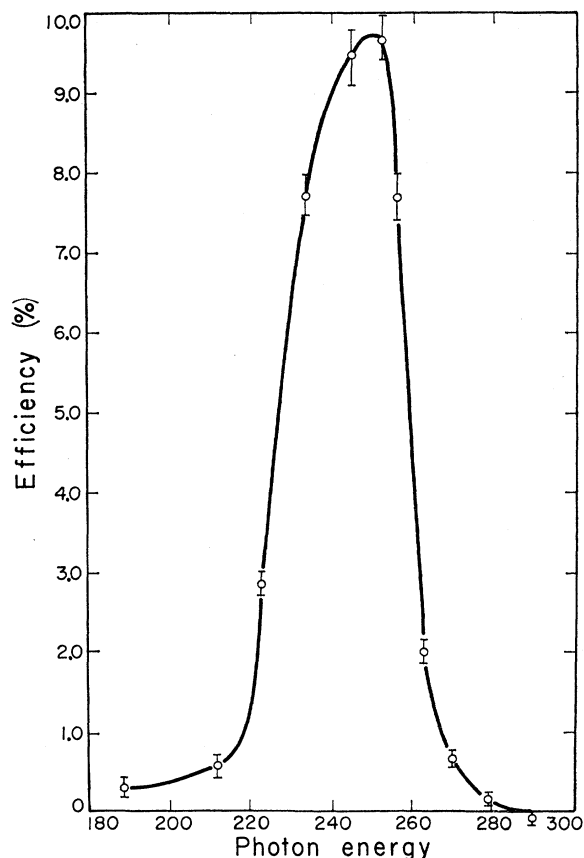


FIG. 2. The selected photon spectrum. Plot of the efficiency of the electron counter for counting electrons vs the energy of the associated gamma ray. Curve drawn for illustrative purposes only.

counter placed so that it observed only electrons associated with 245 ± 15 -Mev gamma rays. This counter consisted of a plastic scintillator $1\frac{3}{8} \times 1\frac{3}{8} \times 4$ in. viewed by a 1P21 photomultiplier tube. The 1P21 was surrounded by a triple iron magnetic shield and about 6 in. of lead. The counter was calibrated by means of a pair spectrometer. The spectrum of gamma rays selected had, as shown in Fig. 2, a peak at 245 Mev and a full width at half maximum of 30 Mev. The improved resolution was due principally to the thin window on the inside wall of the vacuum chamber.

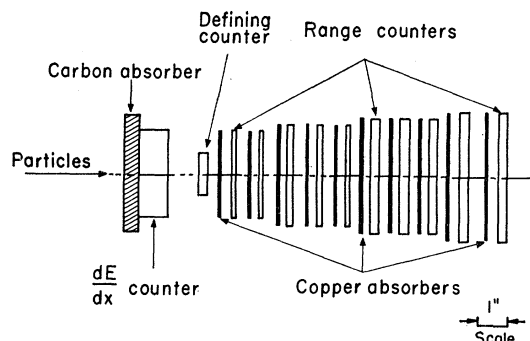


FIG. 3. Proton telescope geometry. All counters are plastic scintillator.

A somewhat disturbing feature of the electron counter was that it had only 10% efficiency for counting electrons. Tests indicated that the iron magnetic shield was not adequate. However, because the counter was already an imposing structure and because we thought that more iron might perturb the synchrotron magnetic field so that it would be difficult to obtain a beam of electrons, we decided to perform the experiment with the counter as it existed rather than to enlarge it.

The residual electrons whose orbits allowed them to enter the electron counter had an energy of 90 ± 5 Mev. Since this energy was so well defined, any fluctuation in the electron counter efficiency could not change the spectrum of selected photons. Also, since the whole energy spectrum of protons was observed simultaneously by a multichannel proton telescope, changes in the efficiency of the electron counter could not affect the shape of this spectrum. It could, however, have introduced an error into the absolute magnitude of the results. The efficiency was observed, nevertheless, to be quite constant.

The proton telescope geometry is shown in Fig. 3. It consisted of (a) a small scintillator to define the solid angle, (b) a large scintillator to measure dE/dx , and (c) a series of 10 scintillators, separated by copper absorbers.⁵ These scintillators and absorbers divided the energy region from 90–250 Mev into nine intervals. The first four intervals were 15 Mev each and the last five were 20 Mev each.

A triple coincidence between the dE/dx counter, the defining counter, and the electron counter was used to trigger a 517 Tektronix oscilloscope. The resolving time of the coincidence circuit was 3 μ sec. The signals from the range counters and the dE/dx counter were tapped onto a coaxial delay line so that they could be consecutively displayed on the oscilloscope. The traces were then photographed on 35-mm film.

III. TREATMENT OF THE DATA

The events were entered on a plot of the pulse height from the dE/dx counter vs the number of range counters

⁵ Dwight R. Dixon, University of California Radiation Laboratory Report UCRL-2956, 1955 (unpublished).

TABLE I. Corrections to proton spectrum.

	1	2	3	Range interval			7	8	9
	4	5	6						
Correction (%) due to range straggling in absorbers	1.4	5.9	7.4	8.8	12.6	15.8	18.5	20.9	33.0
Correction (%) due to scattering in parent nucleus	11	11	11	11	9	9	7	7	7

traversed. Protons were identified by their characteristic separation from meson and electron events, on such plots as described in detail elsewhere.^{5,6}

To keep accidental counts reasonably low, it was necessary to operate the synchrotron at about 1% of full beam intensity. This corresponded to 2×10^7 equivalent quanta per minute. Events were recorded at the rate of 6 per hour. Of these, analysis showed that 3 per hour were protons and the remainder, mesons and electrons. Of the protons, 1 per hour was an accidental. A total of 694 protons was observed, of which 248 were accidentals.

To determine the number of accidentals, runs were taken with the electron counter pulses delayed by a time equal to one revolution time of the electrons in the accelerator. Runs with and without the added delay were alternated every 2 hr (about 50 times) throughout the experiment. The accidental runs were normalized to the real runs by means of a thick-walled ionization chamber of the Cornell type placed in the gamma-ray beam.

The proton spectrum was corrected for (a) range straggling of the protons in the telescope due to nuclear collisions in the proton telescope absorbers, (b) energy loss of the protons due to collisions with other nucleons before leaving the parent nucleus, and (c) ionization energy loss of the protons in the target. The first correction was measured at the 184-in. cyclotron by placing the proton telescope in a monoenergetic beam of protons with various select energies. The second correction was calculated by using the approximate method of Weil and McDaniel.² The third correction was readily determined from the projection of the thickness of the target onto the direction of the proton telescope. The results of the first two corrections are shown in Table I.

The cross section was calculated from the formula

$$N = \frac{d^2\sigma}{d\Omega dE_p} f t \Delta\Omega \Delta E_p, \quad (1)$$

where N = number of events in a given energy interval, f = number of selected photons, $\Delta\Omega$ = solid angle, ΔE_p = width of the given energy interval, and t = thickness of the target, in atoms/cm².

The solid angle of the proton telescope was 0.0276 steradian, the solid angle subtended by the defining

⁶ Robert J. Cence, thesis, University of California Radiation Laboratory Report UCRL-8921, 1959 (unpublished).

counter. The carbon target had an effective thickness of 2.21×10^{23} /cm².

The flux of selected photons was determined from the previously measured efficiency of the electron counter and the total flux of photons, the latter being measured by a thick-walled ionization chamber of the Cornell type.

IV. RESULTS

The cross section calculated from Eq. (1), after the corrections of Table I have been made, and the accidentals subtracted, is shown in Fig. 4. The errors indicated are the probable errors due to statistical uncertainty only. The curves will be explained later.

In Fig. 5 is shown a similar measurement of the differential cross section per equivalent quantum per nucleus for photoproton production from 342-Mev bremsstrahlung. No analysis of these data was made; they are shown for comparison only.

Two features of the data in Fig. 4 should be noted. One is the large high-energy tail in the proton spectrum. The other is the sharp maximum in the spectrum at about 120 Mev. The evidence for the latter rests primarily on the point at 105 Mev. If the efficiency of the first range counter in the proton telescope happened to be lower than the others, the first point would be too low, showing a false peak at the next point. This does not seem likely, for two reasons. First, all the counters appeared to have 100% efficiency. Furthermore, the proton spectrum observed with the full bremsstrahlung spectrum of gamma rays showed no indication of a reduced efficiency in the first counter as can be seen from Fig. 5.

V. THEORY. CALCULATION OF THE CROSS SECTION

We now want to calculate the cross section implied by a given center-of-mass momentum distribution of neutron-proton pairs in the nucleus.

Using the quasi-deuteron model, we calculate the cross section from the kinematics of deuteron photodisintegration and then perform an appropriate average over the motions of all neutron-proton pairs in the nucleus. The resulting expression is

$$\sigma = \int \frac{dn_\gamma}{dE_\gamma} (1 - \beta_{zD}) \frac{d^3N_D d\sigma_D}{dP_D^3 d\Omega_p} \delta(E_\gamma - B - E_p - E_n) \times \delta^3(\mathbf{P}_\gamma + \mathbf{P}_D - \mathbf{P}_n - \mathbf{P}_p) d^3P_D d^3P_n dE_p dE_\gamma. \quad (2)$$

where σ =total cross section per photon per nucleus for the production of protons via the quasi-deuteron process; dn_γ/dE_γ =the energy spectrum of selected photons, normalized to one gamma ray; β_{zD} =the velocity of the quasi-deuteron, in units of the velocity of light, in the z direction (this is the direction assumed for the incoming photons); d^3N_D/dP_D^3 =the momentum probability distribution of quasi-deuterons inside the nucleus, normalized to NZ , the total number of such pairs in the carbon nucleus; $d\sigma_D/d\Omega_p$ =the experimental differential cross section in the laboratory system for the photodisintegration of quasi-deuterons moving inside the nucleus; E_p, P_p, E_n, P_n =the kinetic energy and momentum of the final proton and neutron, respectively, after leaving the nucleus; B =the average effective binding energy of the neutron-proton pair in the nucleus. The factor $(1-\beta_{zD})$ corrects for the Doppler shifting of the photon flux.

The four delta functions in Eq. (2) ensure conservation of energy and momentum. It can be seen that the form of Eq. (2) evidently assumes that the energy and momentum of the final neutron and proton do not change as they leave the nuclear potential well. Refraction at the nuclear surface is thus ignored.

The finite aperture (± 8 deg) of the proton telescope is also ignored. Equation (2) thus yields, by differentiation:

$$\frac{d^2\sigma}{dE_p d\Omega_p} = \int \frac{dn_\gamma}{dE_\gamma} (1-\beta_{zD}) \frac{d^3N_D}{dP_D^3} \frac{d\sigma_D}{d\Omega_p} \delta(E_\gamma - B - E_p - E_n) \times \delta^3(\mathbf{P}_\gamma + \mathbf{P}_D - \mathbf{P}_n - \mathbf{P}_p) dE_\gamma d^3P_D d^3P_n, \quad (4)$$

where $d^2\sigma/dE_p d\Omega_p$ =the differential cross section per photon per nucleus for photoproton production.

The differential cross section (lab) for the photodisintegration of a quasi-deuteron moving inside the

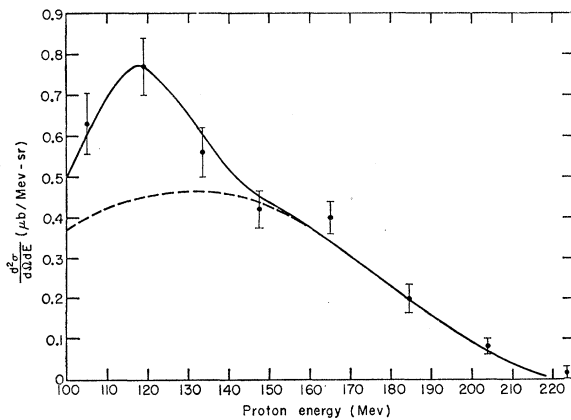


FIG. 4. Experimental results. Plot of the differential cross section per nucleus per selected photon for photoproton production from carbon at 60 deg by 245 ± 15 Mev photons. The curves are explained in the text.

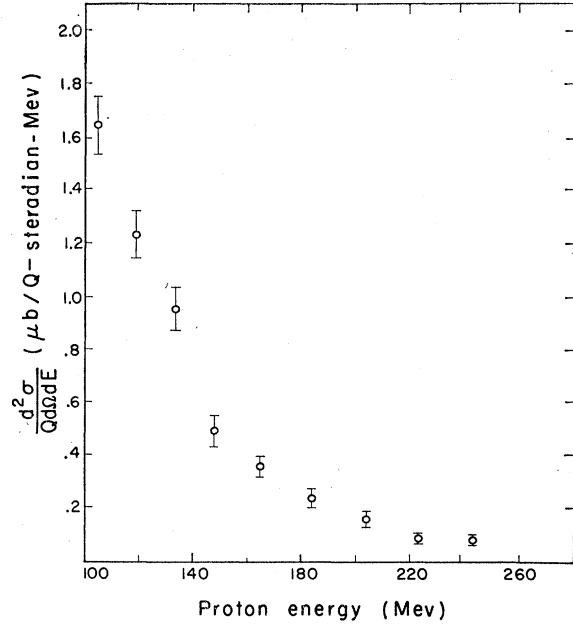


FIG. 5. Plot of the differential cross section per nucleus per equivalent quantum for photoprotons produced at 60 deg by 342-Mev bremsstrahlung on carbon.

nucleus is taken as

$$d\sigma_D/d\Omega_p = (r_I/r_C)^3 (d\sigma_D/d\Omega_p)_{\text{free}}, \quad (5)$$

where r_I =the radius of interaction, r_C =the radius of the carbon nucleus, and $(d\sigma_D/d\Omega_p)_{\text{free}}$ =the differential cross section (lab) for the photodisintegration of a free, moving deuteron. It is a complicated function of E_γ , \mathbf{P}_D , θ_p , and ϕ_p , where θ_p and ϕ_p are the lab angles of the proton.

The factor $(r_I/r_C)^3$ represents the probability that a neutron and a proton will be close enough to participate in the absorption of a photon. This quantity together with the normalization of d^3N_D/dP_D^3 gives the familiar NZ/A dependence of the cross section. The r_I/r_C is left as a free parameter in the calculation.

The $(d\sigma_D/d\Omega)_{\text{free}}$ is first determined in the rest system of the quasi-deuteron. This corresponds to the laboratory system in the usual experiments on photodisintegration of deuterium. It is approximated as⁷

$$(d\sigma_d/d\Omega_p^R)_{\text{free}} = 6.7 + 4.6 \cos\theta_{\gamma p}^R \mu\text{b/sr}. \quad (6)$$

The superscript R indicates variables in the rest system of the deuteron. The cross section is assumed to be independent of energy. To transform to the laboratory system, it is necessary to transform $\cos\theta_{\gamma p}^R$ and multiply the cross section by the appropriate Jacobian.

By virtue of the threefold momentum δ function in Eq. (4), the integrations over P_n can be performed. One more integration can be carried out by using the energy δ function. This is chosen to be the integration

⁷ D. R. Dixon and K. C. Bandtel, Phys. Rev. **104**, 1730 (1956).

over θ_D , the polar angle of the quasi-deuteron. These integrations are shown in the Appendix. The result at $\phi_p = 90$ deg is,

$$\frac{d^2\sigma}{dE_p d\Omega_p} = \frac{E_\gamma - B + E_p + M}{(E_\gamma^2 - E_\gamma P_p + P_p^2)^{\frac{1}{2}}} \int dE_\gamma \int_{P_{\min}}^{P_{\max}} dP_D \times \int_0^{2\pi} d\phi_D \frac{dn_\gamma}{dE_\gamma} (1 - \beta_{zD}) P_D \frac{d^3 N_D}{dP_D^3} \frac{d\sigma_D}{d\Omega_p}. \quad (7)$$

We have put velocity of light = 1.

The integrations in Eq. (7) were done numerically by an IBM 650 computer. The limits P_{\min} and P_{\max} are given by Eq. (A9) in the Appendix.

It should be noted that the form of the energy δ function in Eq. (4) assumes that the quasi-deuteron has constant binding energy in the nucleus. This is perhaps the most suspect assumption in the calculation. Because of this, the relative kinetic energy of the proton and neutron of the quasi-deuteron never appear in the equations for the conservation of energy and momentum. This is because there are only two particles in the final state. It is assumed in the quasi-deuteron model that the incoming gamma ray transfers all its momentum and energy to a single neutron-proton pair. Any excitation energy received by the residual nucleus arises because the final neutron and proton undergo collisions before leaving the nucleus.

VI. DISCUSSION AND CONCLUSIONS

The momentum distribution needed to fit the data was found by trial and error, using Eq. (7). The solid curve in Fig. 4, which we consider to be a good fit to the data, results from the following quasi-deuteron momentum distribution:

$$\frac{d^3 N}{dP_D^3} = \frac{0.2}{(4\pi M E_1)^{\frac{3}{2}}} \exp\left(-\frac{P_D^2}{4M E_1}\right) + \frac{0.8}{(4\pi M E_2)^{\frac{3}{2}}} \exp\left(-\frac{P_D^2}{4M E_2}\right), \quad (8)$$

where $E_1 = 1.6$ Mev, $E_2 = 20$ Mev, and the distribution is normalized to one neutron-proton pair.⁸ To give the proper magnitude we must set $r_I/r_C = 0.38$; and to make the calculated spectrum reach a maximum at the same energy as observed in this experiment, it is necessary to set $B = 40$ Mev.

If we omit the first term in Eq. (8), the proton spectrum is given by the dashed line in Fig. 4. The second term in Eq. (8) is in agreement with previous work, if we assume that neutrons and protons are randomly distributed in the nucleus.⁹ It is clear,

⁸ In a previous report on this experiment (reference 6) an error was made in calculation which precluded satisfactory agreement with the experimental data.

⁹ J. B. Cladis, W. N. Hess, and B. J. Moyer, Phys. Rev. **87**, 425 (1952).

however, that both terms in Eq. (8) are necessary. The proton spectrum with the first term omitted definitely disagrees with the experimental spectrum. One can conclude that there are considerably more low-momentum neutron-proton pairs than would be given by a random distribution of neutrons and protons.

Because the Berkeley synchrotron is no longer in operation, it is not possible for us to extend the work begun here. However, it is hoped that our results will stimulate others to do so. We feel that selected photons have proven themselves useful for probing nuclear internal momenta.

APPENDIX

Equation (4) in the text can be integrated immediately to give

$$\frac{d^2\sigma}{dE_p d\Omega_p} = \int \frac{dn_\gamma}{dE_\gamma} (1 - \beta_{zD}) \frac{d^3 N_D}{dP_D^3} \frac{d\sigma_D}{d\Omega_p} \times \delta(E_\gamma - B - E_p - (P_n^2 + M^2)^{\frac{1}{2}}) d^3 P_D dE_\gamma, \quad (A1)$$

where

$$P_n^2 = P_\gamma^2 + P_D^2 + P_p^2 + 2(\mathbf{P}_\gamma \cdot \mathbf{P}_D - \mathbf{P}_\gamma \cdot \mathbf{P}_p - \mathbf{P}_D \cdot \mathbf{P}_p). \quad (A2)$$

Remembering that \mathbf{P}_γ defines the direction of the polar axis, we can write

$$\frac{d^2\sigma}{dE_p d\Omega_p} = \int \frac{dn_\gamma}{dE_\gamma} (1 - \beta_{zD}) \frac{d^3 N}{dP_D^3} \frac{d\sigma_D}{d\Omega_p} \times \delta(a - (b + 2cP_D + P_D^2)^{\frac{1}{2}}) P_D^2 dP_D \times \cos\theta_D d\phi_D dE_\gamma, \quad (A3)$$

where

$$\begin{aligned} a &= E_\gamma - B + E_p + M, \\ b &= P_\gamma^2 + P_p^2 + M^2 - 2\mathbf{P}_\gamma \cdot \mathbf{P}_p \cos\theta_p, \\ c &= (1/P_D)[P_\gamma \cos\theta_D - P_p \cos\theta_D \cos\theta_p \\ &\quad - P_p \sin\theta_p \sin\theta_D \cos(\phi_D - \phi_p)]. \end{aligned} \quad (A4)$$

We now perform a rotation of the quasi-deuteron coordinates in the lab system:

$$\begin{aligned} x_D &= x_D', \\ y_D &= y_D' \cos\psi - z_D' \sin\psi, \\ z_D &= z_D' \cos\psi + y_D' \sin\psi, \end{aligned} \quad (A5)$$

where

$$\cos\psi = a/(a^2 + b^2)^{\frac{1}{2}}.$$

In the rotated coordinate system

$$c = \alpha \cos\theta_D', \quad (A6)$$

where

$$\alpha = (E_\gamma^2 - E_\gamma P_p + P_p^2)^{\frac{1}{2}}, \quad (A7)$$

and where we have assumed $\phi_p = 90$ deg. Putting Eqs.

(A5) and (A6) into (A3) and integrating over $\cos\theta_D'$, we have Eq. (7) in Sec. V.

In order that the integral in Eq. (A3) $\neq 0$, we must have

$$(b - 2\alpha P_D + P_D^2)^{\frac{1}{2}} \leq a \leq (b + 2\alpha P_D + P_D^2)^{\frac{1}{2}}. \quad (\text{A8})$$

P_{\min} and P_{\max} are deduced from Eq. (A8). The results are

$$\begin{aligned} P_{\min} &= |\alpha - (\alpha^2 - \mu)^{\frac{1}{2}}|, \\ P_{\max} &= \alpha + (\alpha^2 - \mu)^{\frac{1}{2}}, \end{aligned} \quad (\text{A9})$$

where

$$\mu = 4ME_p + 2E_\gamma(-\frac{1}{2}P_p + E_p - M) + 2B(E_\gamma - E_p + M).$$

ACKNOWLEDGMENTS

We would like to thank Gilbert Mead for his generous assistance in the final stages of the experiment, and Rudin Johnson and the synchrotron crew for their enthusiastic cooperation in carrying out the many unusual requests made in connection with this experiment.

Photodissociation of the μ Meson

M. E. EBEL* AND W. D. WALKER†
University of Wisconsin, Madison, Wisconsin

(Received May 26, 1960; revised manuscript received March 6, 1961)

The cross section for the production of a charged vector boson by the dissociation of a high-energy μ -meson beam undergoing Coulomb scattering has been calculated. The cross section for such a process is $(1-3) \times 10^{-34}$ cm² in Pb. Possible experiments for the detection of such decays are discussed.

IN the papers of Good and Walker¹ the possibility of the photodissociation and diffraction dissociation of high-energy beam particles is pointed out. In general, the study of photoprocesses serves as a complement to other means of study of strong interactions (e.g., π -meson scattering vs photoproduction). Thus, so far as the strong interactions are concerned, the Coulomb disintegration will probably serve as a complementary tool to diffraction dissociation. In the case, however, of weak interactions, the Coulomb disintegration of beam particles may be one of the few tools other than a study of decay processes available for probing the nature of the weakly interacting particles. The μ meson is probably the most enigmatic of the fundamental particles and, consequently, the ability to photodissociate the μ meson represents an exciting possibility. We have made a calculation of the photodissociation of the μ meson using a specific model. The model is the one in which the weak interactions are mediated by a charged vector boson.^{2,3} This calculation is much simpler than the corresponding ones for strongly interacting particles, since presumably one may apply the usual perturbation theory treatment to the problem.

The cross section for the production of the intermediate boson and a neutrino by unpolarized μ mesons

of energy E incident on a nucleus of charge Ze has been calculated using the Weizsäcker-Williams approximation. Accordingly, the cross section for photoproduction of B (vector boson) and neutrino by a photon of momentum q incident upon a μ meson at rest has first been calculated in lowest-order perturbation theory for both the weak boson-lepton interaction and the electromagnetic interaction. The result is

$$\begin{aligned} \sigma(q) &= a(q)(\lambda - 2)^2 + b(q)(\lambda - 1) + c(q), \\ a(q) &= (\alpha g^2 / 32 M_B^2) (\ln x + \frac{1}{2} - x^{-1} \ln x - x^{-1} + \frac{1}{2} x^{-2}), \\ b(q) &= (\alpha g^2 / 8 M_B^2) (2 - 3x^{-1} \ln x - x^{-1} - 2x^{-2}), \\ c(q) &= (\alpha g^2 / 8 M_B^2) (-x^{-1} \ln x + 3x^{-1} - 2x^{-2} \ln x \\ &\quad - 2x^{-3} \ln x - 3x^{-3}), \end{aligned} \quad (1)$$

with M_B the boson mass and λ the total magnetic moment of the boson. Here $x = q/q_m$ is the photon momentum in units of the threshold momentum q_m . Note that the cross section diverges for large q unless $\lambda = 2$. The threshold momentum q_m is given by

$$q_m = M_B^2 / 2m,$$

with m the μ -meson mass. The boson-lepton interaction is taken as

$$\mathcal{L}_{B-l} = -g \bar{\psi}_\mu \gamma_\rho \varphi_{\rho 2}^{\frac{1}{2}} (1 + \gamma_5) \psi_\nu + \text{H.c.} + \text{electron terms},$$

so that the coupling constant g is determined by

$$g^2 / M_B^2 = 4 \times 10^{-5} / M_\pi^2. \quad (2)$$

Various terms of order m^2 / M_B^2 relative to the main terms in Eq. (1) have been dropped.

* Supported in part by the Sloan Foundation and a U. S. Atomic Energy Commission contract.

† Supported in part by a U. S. Atomic Energy Commission contract and the Wisconsin Alumni Research Foundation.

¹ M. L. Good and W. D. Walker, Phys. Rev. **120**, 180, 1855 (1960).

² H. Yukawa, Revs. Modern Phys. **21**, 474 (1949).

³ R. P. Feynman and M. Gell-Mann, Phys. Rev. **109**, 193 (1958); J. Schwinger, Ann. Phys. **2**, 407 (1957).